WAVE EFFECTS IN 6DOF ON A SHIP IN SHALLOW WATER

Manases Tello Ruiz, Ghent University, Maritime Technology Division, Belgium.

Stefaan De Caluwé, Ghent University, Maritime Technology Division, Belgium.

Thibaut Van Zwijnsvooorde, Ghent University, Maritime Technology Division, Belgium.

Guillaume Delefortrie, Flanders Hydraulics Research, Belgium.

Marc Vantorre, Ghent University, Maritime Technology Division, Belgium.

SEVERAL AUTHORS HAVE RECENTLY STUDIED MANOEUVRING CONSIDERING THE MORE GENERAL CASE OF SHIP MOTION IN SIX DEGREES OF FREEDOM AND INCORPORATING WAVE EFFECTS INTO THE ANALYSIS. WAVE FORCES AND WAVE-INDUCED MOTIONS HAVE BEEN TAKEN INTO ACCOUNT BY COMBINING THE CONVENTIONAL ANALYSIS OF BOTH SEAKEEPING AND MANOEUVRING. HOWEVER, THOSE STUDIES MOSTLY FOCUS ON DEEP WATER SCENARIOS. SHALLOW WATER CONDITIONS, WHICH OCCUR IN ACCESS CHANNELS TO HARBOURS, HAVE A SUBSTANTIAL EFFECT ON BOTH WAVE CHARACTERISTICS (E.G. WAVE STEEPNESS, ELLIPTIC ORBITS) AND SHIP BEHAVIOUR (E.G. IMPORTANCE OF SQUAT). AT THE TOWING TANK FOR MANOEUVRES IN SHALLOW WATER (CO-OPERATION FLANDERS HYDRAULICS RESEARCH - GHENT UNIVERSITY), A SYSTEMATIC SERIES OF CAPTIVE MODEL TESTS HAS BEEN EXECUTED WITH A 1/75 SCALE TANKER MODEL OF THE KVLCC2 REFERENCE SHIP. THIS TEST PROGRAM WAS PARTIALLY CARRIED OUT IN THE FRAME OF THE EUROPEAN RESEARCH PROGRAM ENERGY EFFICIENT SAFE SHIP OPERATION (SHOPERA). THE KVLCC2 MODEL WAS SYSTEMATICALLY TESTED IN BOTH CALM WATER AND IN REGULAR WAVES, AND IN TWO DIFFERENT WATER DEPTHS. DURING TESTS DIFFERENT COMBINATIONS OF INCOMING WAVE ANGLE, WAVE AMPLITUDES AND PERIOD WERE USED. THE EFFECTS OF INCIDENT WAVES ON THE MOTIONS, FORCES AND MOMENTS ACTING ON THE SHIP IN THE HORIZONTAL PLANE, AND ITS IMPORTANCE CONSIDERING SHIP MANOEUVRABILITY IN SHALLOW WATER WILL BE DISCUSSED. IN ADDITION, THE EXPERIMENTAL RESULTS WILL BE COMPARED TO NUMERICAL METHODS BASED ON STRIP THEORY AND 3D BOUNDARY INTEGRAL EQUATION METHODS.

Keywords: Drift forces, shallow water, experimental, numerical, KVLCC2.

INTRODUCTION

Several phenomena are experienced when a ship sails in the presence of waves: such as wave induced motions and forces, second order wave forces, and reduction of speed. During the last decades, these wave effects have been a constant subject of study for ships sailing in straight motion and at constant forward speed (seakeeping studies). A counterpart analysis describing the curvilinear motion of ships in restricted waters has been undertaken under the subject of manoeuvring in calm water, where mostly horizontal motion have been studied and wave effects are neglected. The subdivision in two separate studies is to take advantage of the dominant environmental phenomena, however, this is not always a valid assumption. Navigational areas such as access channels to ports are an exception to these simplifications because in such an environment the ship is expected to manoeuvre under wave action.

Wave effects on a manoeuvring ship are also of importance in the frame of new regulations that have been put into force by the International Maritime Organization (IMO) for CO_2 emissions allowance. These new directives have been introduced in order to comply with the mandate from the Kyoto protocol. The directives have been established by the Marine Environment Protection Committee (MEPC) and are expressed by the Energy Efficient Design Index (EEDI), which constrains the maximum installed power on-board.

Considering the new IMO regulations, the reduction of speed is a wave effect that must be taken into account. This effect is understood as an increase of the ship resistance compared to calm water conditions, also known as added wave resistance. The correct estimation of this effect is of critical importance in order to estimate the required engine power to satisfy the designed speed. Several methods addressing this problem have been developed during the last decades, to mention some: Havelock [1], Maruo [2], Joosen[3], Boese [4], Gerritsma and Beukelman [5]. The accuracy of these methods according to Strom-Tejse [6] can be judged as poor for a wide range of ship forms and speeds. Two more general methods, allowing the estimation of the added wave resistance for any ship type, at any speed and heading, have been developed, one by Faltinsen [7], and the other by Salvesen [8].

Indeed, the importance of the added wave resistance cannot be neglected when navigating in waves; in addition, another wave effect of crucial importance is the mean second order wave forces (also known as mean wave drift force). This mean steady component is usually estimated by two main approaches, the near-field and the far-field method. The far-field formulation is preferable in practice thanks to its better convergence and stability. However, the far-field formulation cannot provide the vertical drift loads which can be very important considering shallow water scenarios. Another method, known as middle-field formulation, was proposed by Chen in [9] and Rezende et al. in [10] claiming to overcome the convergence problems of the near field.

Aiming to solve the more general case of manoeuvring in waves for deep water scenarios, recently new methods (e.g. [11], [12] and [13]) have incorporated the horizontal mean wave drift force and added wave resistance into the conventional model of manoeuvring in calm water. Hence, only horizontal steady force components obtained from the seakeeping analysis have been taken into account. This information is introduced into the manoeuvring model every time step (e.g. [14], [15] and [16]) or when a certain criterion is reached (e.g. [13], [17] and [18]). The use of conventional methods attempts to account for the main

phenomena experienced in each independent analysis: viscous and lift type for the manoeuvring in calm water and potential contribution from seakeeping.

Although the new approaches represent an improvement to study manoeuvring in waves, their applicability is constrained to deep water areas. In shallow water scenarios and under the presence of waves, not only the added wave resistance and horizontal mean wave drift forces are of great interest. Taking into account the larger size of the ships and the restriction in depth, as well as the width of access channels, the wave-induced motion, forces and moments, all mean drift force components are relevant to avoid hazards such as grounding and collisions. Hence, the simplifications and assumptions used to develop the current mathematical models have to be compared against experimental data obtained for shallow water scenarios.

To get an insight into the ship motions and forces subjected on the ship by waves in shallow water, a systematic series of captive model tests has been executed with a 1/75 scale model of the KVLCC2 reference ship. This test program was partially carried out in the frame of the European research program Energy Efficient Safe Ship Operation (SHOPERA). The KVLCC2 model was systematically tested in both calm water and in regular waves, and in two different water depths. During tests different combinations of incoming wave angle, wave amplitudes and period were used.

The experimental values are compared against three numerical methods based on strip theory and the 3D boundary integral equation methods. Here, Seaway [19], Hydrostar [20] and Wamit [21] are used. The linear wave motions and forces are compared against Seaway and Hydrostar, the mean horizontal wave drift forces against Hydrostar and Wamit, and the added wave resistance is compared against Seaway.

EXPERIMENTAL PROGRAM

EXPERIMENTAL SETUP

The experimental program was conducted at the towing tank for manoeuvres in shallow water at Flanders Hydraulics Research in Antwerp, Belgium. The towing tank's useful dimensions are 68 by 7 m and the maximum water depth is 0.50 m. The test execution process is highly automated to allow 24/7 performance with an average of 32 tests per day. During tests the ship model was connected to the carriage mechanism, the mechanism allows heave, pitch and roll motions. The carriage mechanism consist of three separate working carriages. The main carriage moves in the longitudinal direction, the lateral carriage moves in the transversal direction and a yawing table rotates the model (see, [22]).

A sketch describing the position of the ship during tests and the definition of the parameters involved is shown in Figure 1. The ship's main characteristics for full scale and model scale are given in Table 1.

To measure the wave amplitudes, forces, and motions, several gauges were employed along the tank and the ship model. Their respective locations in the tank and the ship are displayed in Figure 2. The wave profile is measured at six locations ($WG1 - WG6$), in order to investigate the development of wave amplitude along the tank. The variations observed and reported in [22] are not significant to the desired wave amplitude, especially at larger

L_{PP}/λ ratios, hence a constant wave amplitude along the tank can be assumed. The horizontal forces and the vertical displacements are measured at two ($FG1$ and $FG2$) and four ($DG1$, $DG2$, $DG3$ and $DG4$) positions, respectively, see Figure 2.

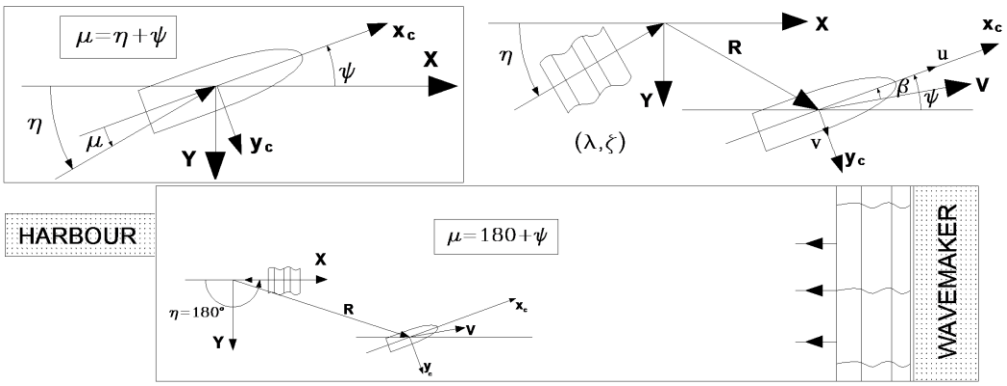

FIGURE 1 – GENERAL POSITION OF THE SHIP DURING TESTS

TABLE 1 – SHIP MAIN CHARACTERISTICS FOR FULL AND MODEL SCALE

		Full scale 1/1	Model scale 1/75
L_{PP}	[m]	320	4.267
B	[m	58	0.773
T_M	[m]	20.8	0.273
V	[m^3]	320438	0.7362
C_b	[-]	0.83	0.81
LCG	[m]	11.1	0.145
GM_T	[m]	5.71	0.179
BM_T	[m]	13.42	0.076
KB_T	[m]	10.87	0.2477
r_{44}	[m]	23.2	0.31
r_{55}	[m]	80	1.07
r_{66}	[m]	80	1.07

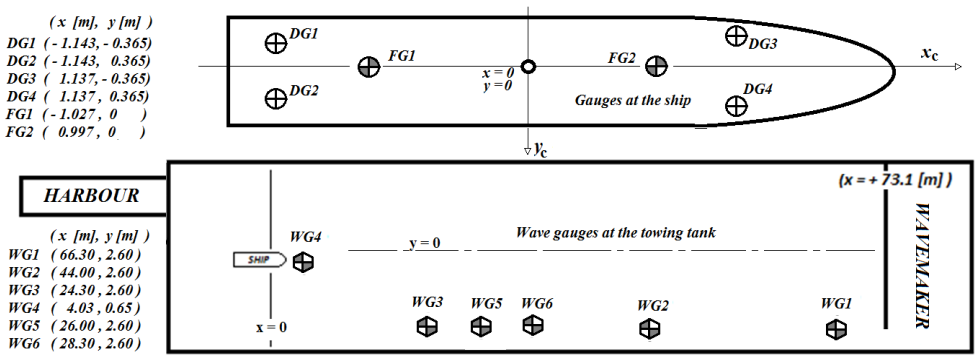

FIGURE 2 – POSITION OF THE INSTALLED WAVE, FORCE AND DISPLACEMENT GAUGES

The experimental program for the KVLCC2 consisted of two main test types. One in head waves ($\mu = 180°$), with and without ship's forward speed ; and the second one at five different incoming-wave angles ($\mu = 30°, 60°, 90°, 120°$, and $150°$), without ship's forward speed. The chosen values for the incoming wave angle, μ, the ship speed, V_S, the wave amplitude, ζ_A, and the water depth, h, are presented in Table 2 and 3.

The executed program comprised three wave amplitudes ζ_{A1} =1.125 and ζ_{A2} =0.75 and ζ_{A3} =1.5 m at full scale. The first and the second amplitude were used for all test at $30\%\ ukc$ and $20\%\ ukc$, respectively. The last one was only employed for $20\%\ ukc$ and V_S=6 knots.

TABLE 2 – TEST MATRIX FOR THE KVLCC2 AT DRAUGHT, $T_m = 20.8$. AT FULL SCALE

$\boldsymbol{\mu}$ [°]	$\boldsymbol{\zeta_A}$ $[m]$	$\boldsymbol{ukc}$ [%]	$\boldsymbol{V_S}$ [knots]	$\boldsymbol{L_{PP}/\lambda}$								
			0	5.00	3.33	2.50	2.00	1.67	1.43	1.25	1.11	1.00
180	1.125	30	6	--	3.33	2.50	2.00	1.67	1.43	1.25	1.11	1.00
			12	--	3.33	2.50	2.00	1.67	1.43	1.25	1.11	1.00
	0.75		0	5.00	3.33	2.50	2.00	1.67	1.43	1.25	1.11	1.00
180	0.75,1.5	20	6	5.00	3.33	2.50	2.00	1.67	1.43	1.25	1.11	1.00
	0.75		12	5.00	3.33	2.50	2.00	1.67	1.43	1.25	1.11	1.00
150			0	5.00	3.33	2.50	2.00	1.67	1.43	1.25	1.11	1.00
120				5.00	3.33	2.50	2.00	1.67	1.43	1.25	1.11	1.00
90	1.125	30		5.00	3.33	2.50	2.00	1.67	1.43	1.25	1.11	1.00
60				5.00	3.33	2.50	2.00	1.67	1.43	1.25	1.11	1.00
30				5.00	3.33	2.50	2.00	1.67	1.43	1.25	1.11	1.00

TABLE 3 – ADDITIONAL TEST MATRIX FOR THE KVLCC2 AT DRAUGHT, $T_m = 20.8$, AT FULL SCALE

$\boldsymbol{\mu}$ [°]	$\boldsymbol{\zeta_A}$ $[m]$	$\boldsymbol{ukc}$ [%]	$\boldsymbol{V_S}$ [knots]	$\boldsymbol{L_{PP}/\lambda}$								
			0	--	1.54	1.33	--	--	--	0.91	--	0.83
180	1.125	30	6	--	--	--	--	--	--	0.91	--	0.83
			12	1.82	--	--	--	--	--	0.91	--	0.83
	0.75		0	1.82	1.54	1.33	1.18	1.05	0.95	0.91	0.87	0.83
180	0.75,1.5	20	6	1.82	1.54	1.33	1.18	1.05	0.95	0.91	0.87	0.83
	0.75		12	--	1.54	1.33	1.18	1.05	0.95	0.91	0.87	0.83

The variation of the ukc was achieved by decreasing the water depth, hence the under keel clearances of 30% ukc and 20% ukc correspond to water depths of $\mathrm{h} = 27.04$ and $\mathrm{h} = 24.96$ m, respectively. Although all given combinations of waves presented in Table 2 and 3 were tested, the results obtained for the ones shaded will not be displayed because of the lack of stationary response observed during the test.

ANALYSIS OF THE EXPERIMENTAL DATA

From the raw data measured during tests, a useful interval where a steady behaviour of the ship is observed has to be selected. Here, a steady signal is defined as one with a (more or less) constant mean value and amplitude of motions and forces over a span of time. Emphasis must be made on ‘more or less' as these are experimental results and as such the results will never be completely ideal. Figure 3 shows an example of the selected time interval.

After the interval selection, the amplitudes of the motions and force time series have to be extracted. These values are needed to compute the linear motions and forces, as well as the

second order wave forces. This has been conducted with a regression analysis with the based formulation composed of a constant term and three harmonics, see Equation 1.

$$f(t) = a_0 + a_1\cos(\omega t) + b_1\sin(\omega t) + a_2\cos(2\omega t) + b_2\sin(2\omega t) + a_3\cos(3\omega t) + b_3\sin(3\omega t)$$

EQUATION 1

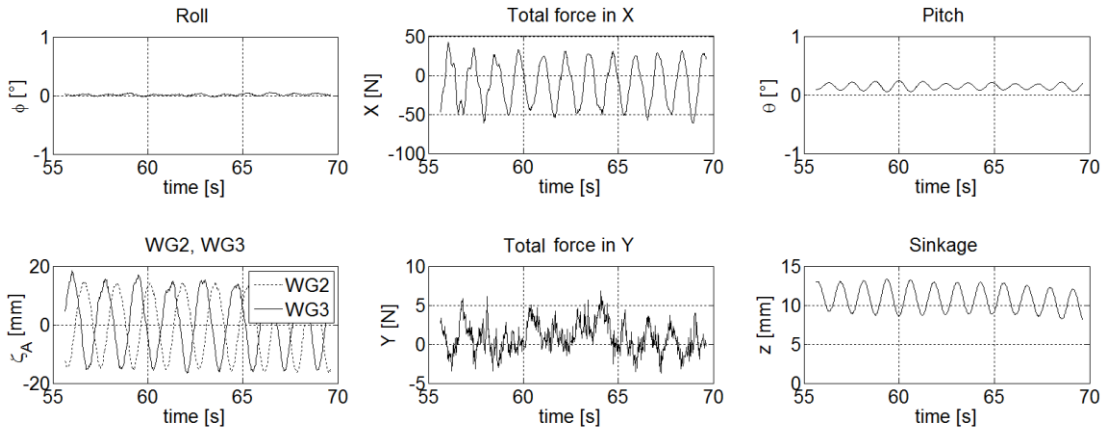

FIGURE 3 – EXAMPLE OF THE TIME WINDOW SELECTED FROM THE RECORDED TIME SERIES

EXPERIMENTAL AND NUMERICAL RESULTS

NUMERICAL MODELS

For the present study, the numerical packages of Seaway, Hydrostar and Wamit have been employed. For Seaway the geometry input consists of section offsets, and for the panel methods the ship is discretised in panels. It is known that the results of the panel method are dependent on the size of the mesh. A suggested panel size in Wamit is of $1/8th$ of the characteristic wave length, however this discretization is not always possible due to computational capacity limits. In the present study, a convergence study was carried out, based on linear wave motions and forces, resulting in a final discretization of 2400 and 4800 panels for Hydrostar and Wamit, respectively (see Figure 4).

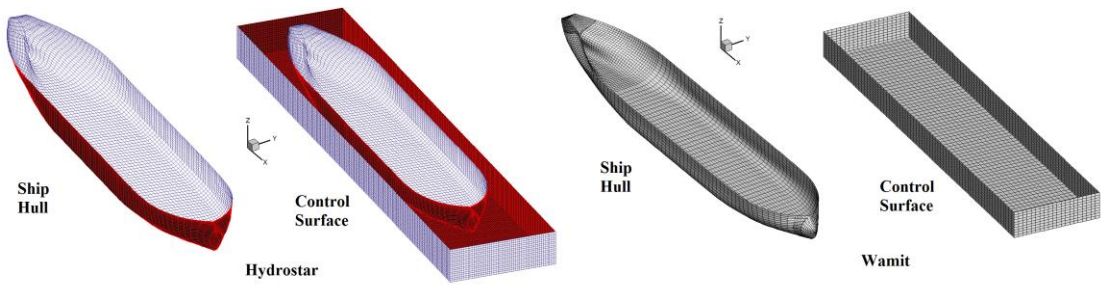

FIGURE 4 –HYDROSTAR AND WAMIT MESHES OF THE HULL AND CONTROL SURFACES

LINEAR WAVE INDUCED MOTIONS

When the ship navigates in shallow water scenarios and in the presence of waves, the developed wave-induced motions are a major concern because of the limited water depth. To understand the ship behaviour in such conditions, and to determine the applicability of potential codes regarding harmonic motions, the comparison between the numerical and the experimental linear response amplitude operator (RAO) are shown in Figures Figure 5, Figure 6, and Figure 7.

In Figure 5 the RAOs for heave and pitch are plotted for three different speeds, in head waves ($\mu = 180°$), and $30\%\ ukc$. The experimental values are compared against the numerical packages of Seaway, Hydrostar, and Wamit (Wamit can only be used for the zero speed case). The results are arranged in a non-dimensional form, and as a function of the ratio L_{PP}/λ of the ship length (L_{PP}) and the wave length (λ).

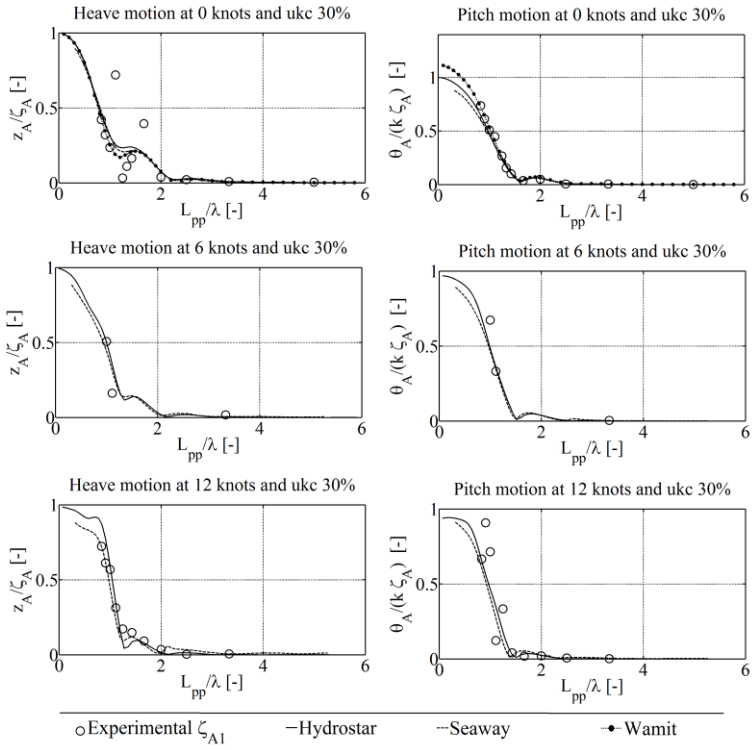

FIGURE 5 –EXPERIMENTAL AND NUMERICAL RAOS IN HEAVE AND PITCH, AT $30\%\ ukc$, $\mu = 180°$. AND THREE DIFFERENT SPEEDS

From Figure 5, it is observed that the numerical codes present similar results for all the study cases, and their estimations predict the responses in heave and pitch with a good approximation. The experimental values follow the trend of the numerical codes with two clearly defined regions, one ranging from $L_{PP}/\lambda \approx 0$ to $L_{PP}/\lambda \approx 2$, and a second one starting from $L_{PP}/\lambda \approx 2$. In the first one the ship moves with larger amplitudes while in the second one the ship seems undisturbed by the wave action. In addition; it is observed that the responses are flattened as the ship increases speed.

The results obtained at five different wave incidence angles ($\mu = 30°, 60°, 90°, 120°$, and $150°$), $30\%\ ukc$, and zero speed are presented in a non-dimensional form in Figure 6 for heave, pitch and roll motion. And in Figure 7, heave and pitch are compared for three

different speeds, in head waves ($\mu = 180°$), and $20\%\ ukc$; a second wave amplitude was only used for the case when the ship's speed was $6\ knots$.

As observed in Figure 5, the responses in Figure 6 are approximately the same for the numerical codes. Some discrepancies are seen between the theoretical calculations, for example for pitch motion at lower L_{PP}/λ ratios, and for roll motion at resonance frequency ($L_{PP}/\lambda \approx 1$), however they are not significant. These discrepancies are less important when comparing their results against the experimental values. All the numerical packages seem to estimate the responses with a good approximation.

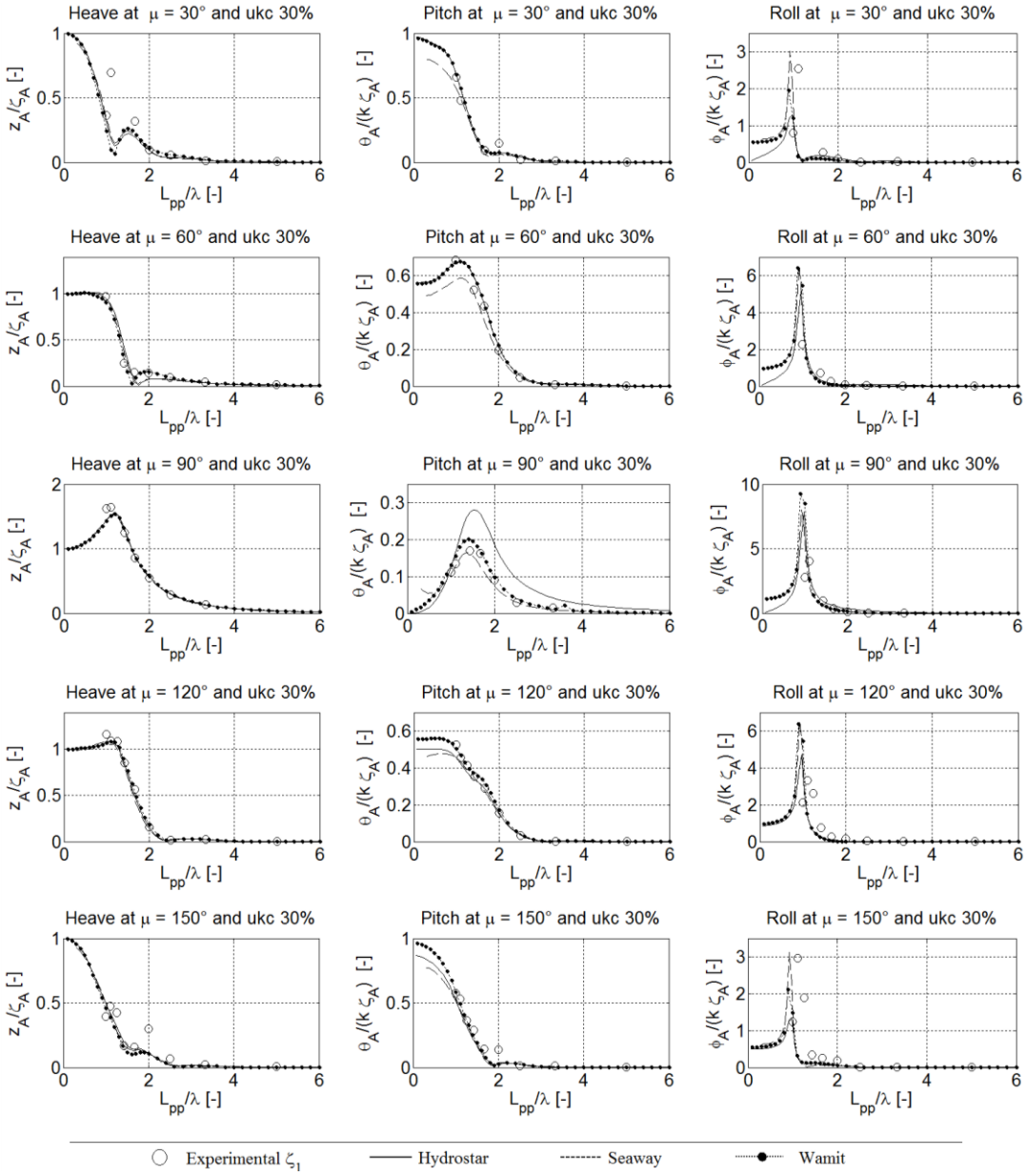

FIGURE 6 –EXPERIMENTAL AND NUMERICAL RAOS IN HEAVE AND PITCH AND ROLL, AT $30\%\ ukc$ AND ZERO SPEED

At $30\%\ ukc$ the predicted linear responses for heave, pitch and roll agree quite well with the experimental ones. The same findings are obtained for heave and pitch (see Figure 7) at $20\%\ ukc$. It is important to point out that even though a higher non-linear effect is expected on the waves at lower ukc, because a larger wave amplitude was used, (see plots at the

middle position in Figure 7), the good agreement of the linear results still holds true at a lower ukc.

From Figures Figure 5, Figure 6, and Figure 7 an agreement between the experimental and the numerical values can be identified, moreover, as discussed above for Figure 5, two regions can be determined separated by the ratio around $L_{PP}/\lambda \approx 2$. The two regions are of great interest since they will delimit the ship-motion response to waves. For the first region the ship will move generating waves, thus the radiation problem will become important, in contrast, in the second region the ship practically will not move due to wave action and the forces arising will be mainly of the Froude-Krylov type.

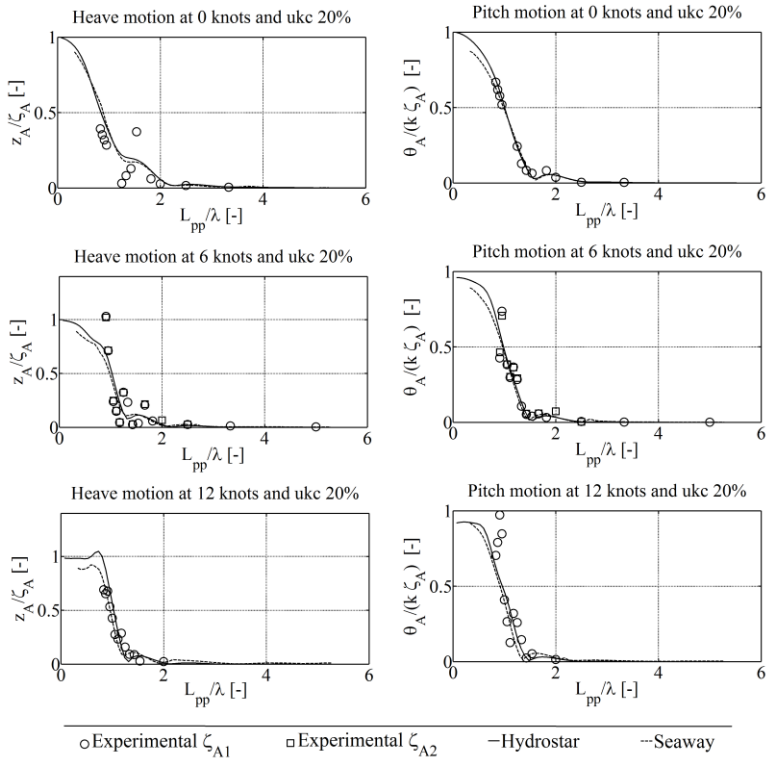

FIGURE 7 –EXPERIMENTAL AND NUMERICAL RAOS IN HEAVE AND PITCH, AT 20% ukc, , $\mu = 180°$, AND THREE DIFFERENT SPEEDS

FIRST ORDER WAVE FORCES

During tests, forces in surge and sway were measured by two force gauges located at the fore and aft of the ship. Then, the moment in yaw was obtained from the combination of the two force gauges (see Figure 2). The results are compared again with the numerical values of Seaway, Hydrostar and Wamit. These first order wave forces and moments are presented in Figure 8, Figure 9, and Figure 10 in a non-dimensional form and as a function of the ratio given by L_{PP}/λ.

From Figure 8 it can be observed that the numerical results are similar for the panel methods in comparison to the one obtained from the strip theory method of Seaway (at zero speed). In addition, the results for the panel methods at zero speed, agree better with the experimental ones. However, when the ship's speed increase, none of the numerical packages predicts the surge forces with a good accuracy.

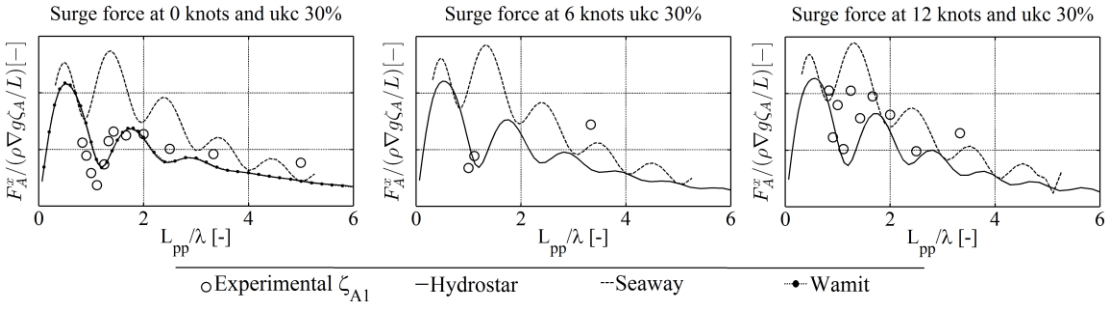

FIGURE 8 – SURGE FIRST ORDER WAVE FORCES IN HEAD WAVES AND AT 30 % *ukc*

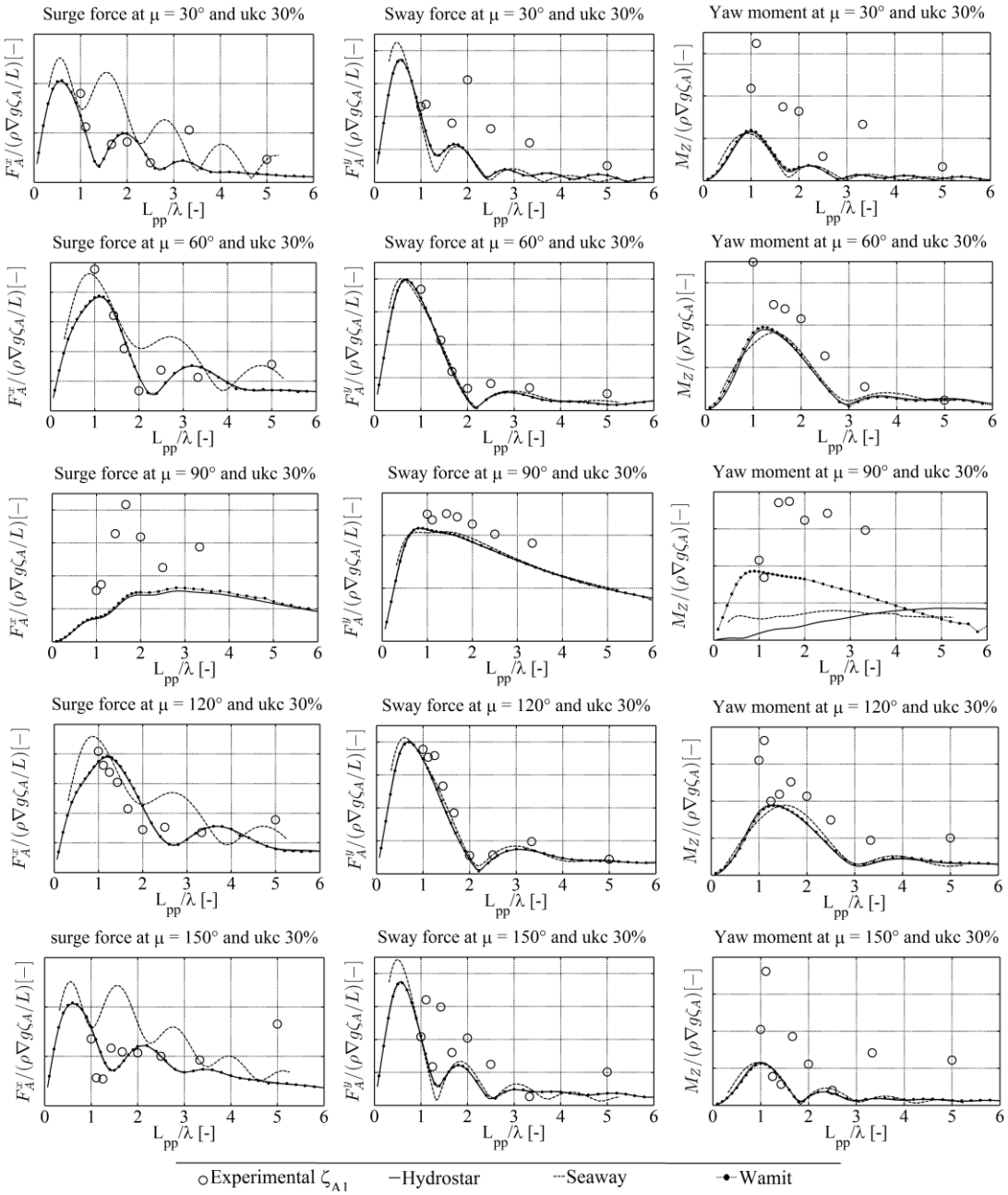

FIGURE 9 – FIRST ORDER SURGE AND SWAY FORCES, AND YAW MOMENT AT ZERO SPEED AND 30% *ukc*

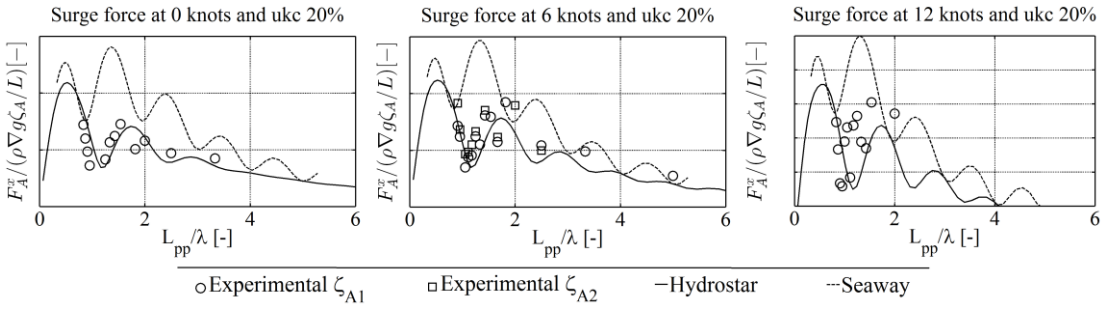

FIGURE 10 – SURGE FIRST ORDER WAVE FORCES IN HEAD WAVES AND AT 20% ukc

At zero forward speed (Figure 9) and incoming wave angles ($\mu = 30°, 60°, 90°, 120°$, and $150°$), the surge and sway responses are better predicted by the panel methods. The estimation of the yaw moment, however, does not show the same behaviour; only at incoming-wave angles of $60°$ and $120°$ a better approximation is observed. The larger discrepancies obtained for the moment, can be partly understood when considering the shape of the ship. The large bulky body does not change considerably from fore to aft as a container ship does. Hence, for any wave approaching from the side the measured moment will be small and this could induce in some error when estimating the experimental values.

If a variation of ukc and wave amplitude is considered (see Figure 10), surge forces seem to be practically the same as observed at 30% ukc, with the panel methods predicting better the first order forces and moments.

ADDED WAVE RESISTANCE

The added wave resistance will be compared in the present work against two methods available in Seaway. These methods are the integrated pressure method (PI) and the radiated energy method (GB). Although the accuracy of those approaches is judged as poor ([6]), their use is direct and will help to get an inside of the problems involved when dealing with added wave resistance for shallow water scenarios. The comparisons between the experimental and numerical results for added wave resistance are presented in Figure 11 for an ukc of 30% and 20%, respectively.

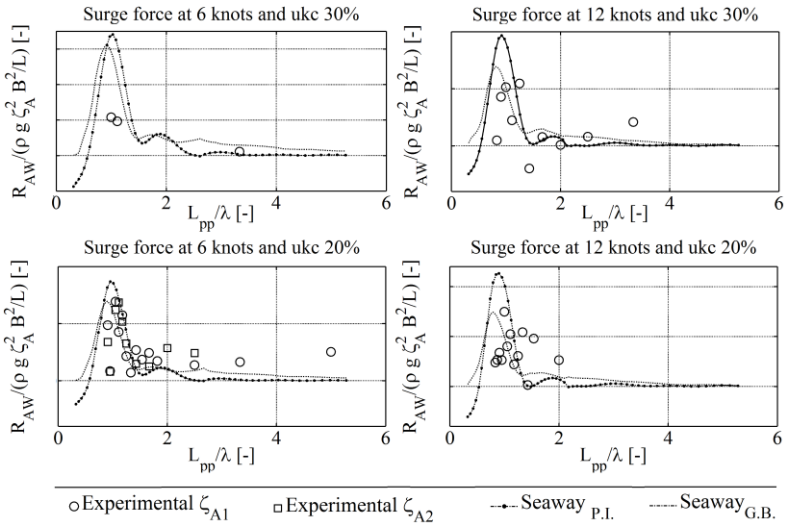

FIGURE 11 –EXPERIMENTAL AND NUMERICAL ADDED WAVE RESISTANCE AT 30% ukc (TOP) AND 20% ukc (BOTTOM)

In Figure 11 only a few points were obtained for the tests at 6 knots and $30\%\ ukc$ in contrast to the ones at 12 knots for the same ukc. For this ukc, the experimental points lay in general closer to the numerical values estimated by the G.B. method. The same is observed for the lower ukc of 20%. The estimation of the added resistance is observed at best for ratios of L_{PP}/λ in the range of $1 < L_{PP}/\lambda < 3$. Large differences observed for $L_{PP}/\lambda > 3$ can be addressed to the neglected effects of the diffraction problem at higher frequencies (See, Journée [19]).

A certain spreading is also observed in the experimental values for $L_{PP}/\lambda < 1$, for all plots shown in Figure 11. This spreading increases with the ship speed. The reason behind this can be associated to the interaction of the radiated waves (generated by large developed motions of the ship) and the towing tank walls. The increased motion response to waves can be confirmed when looking to Figure 5 and Figure 7. In these figures, the ship motions for heave and pitch increase for ratios of $L_{PP}/\lambda < 1$ and at larger ship speeds.

Considering the shallow water scenario, the limited range of frequencies, L_{PP}/λ >1 and $L_{PP}/\lambda < 3$, and small values of the ship speed, the GB used in Seaway can be employed to estimate the added wave resistance. Evaluations out of this range is, however, limited due to non-linear effects associated to the variation of the wetted surface, the flow around the ship hull and the ship motions.

MEAN SECOND ORDER WAVE FORCES

The experimental results are compared against the numerical values obtained from Hydrostar and Wamit. Three different approaches to estimate the drift forces for each package are used: for Hydrostar the near field(N.F.), the middle filed (M.F.) and the far field(F.F.); and for Wamit the pressure integration(P.I), the momentum integration (M.I), and the momentum flux on a control surface (C.S.). The results are displayed in Figure 12. Only horizontal drift forces in surge, sway and yaw are presented for five different incoming-wave angles.

From Figure 12 the first observation is regarding the congruence of the numerical results. Wamit presents bigger differences between, increasing as function of L_{PP}/λ. In contrast, Hydrostar shows minor differences between its three numerical approaches. The higher fluctuation of the results obtained from Wamit can be addressed to irregular frequencies and the mesh size. From another point of view, this shows an advantage of Hydrostar in respect because the amount of panels used in Hydrostar is even less than the ones employed in Wamit.

It can also be observed from Figure 12 that none of the numerical calculations seems to predict with a good accuracy the experimental values for a wide range of L_{PP}/λ ratios. Only Hydrostar results for surge and sway forces at larger values of L_{PP}/λ , for bow and astern quartering waves, present a good agreement. Regarding the yaw moment, not much can be stated as the non-dimensional values are very small compared to the surge and sway forces. The major discrepancies observed are for $L_{PP}/\lambda < 1.5$, the same behaviour was also observed for the added wave resistance where the ship at such wave excitations develop larger induced-wave motions, see Figure 5.

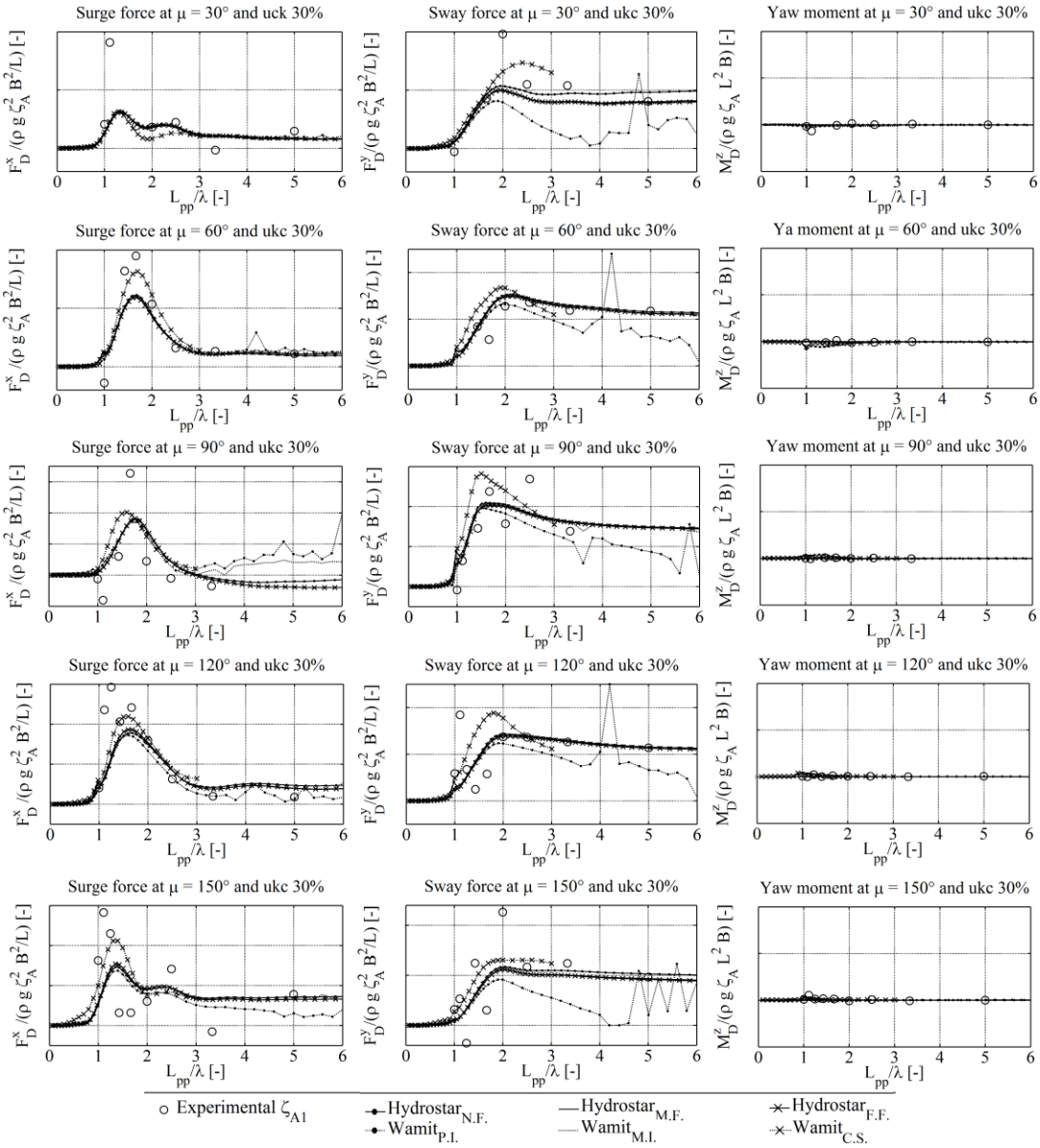

FIGURE 12 –NUMERICAL AND THEORETICAL VALUES FOR THE MEAN WAVE DRIFT FORCES IN SURGE (LEFT) AND SWAY (CENTRE), AND YAW MOMENT (RIGHT)

CONCLUSIONS

To investigate the wave effects in shallow water and determine their importance for the more general case of manoeuvring in waves, a systematic series of captive model tests has been executed with a 1/75 scale tanker model of the KVLCC2 reference ship. During the captive model tests, the KVLCC2 model was systematically tested in both calm water and in regular waves with different combinations of wave amplitudes, headings and periods. In addition, tests at a second water depth were also carried out.

The measured linear motions present a significant amplitudes for waves of lengths up to a ratio of $L_{PP}/\lambda \approx 3$, rapidly decreasing to approximately zero as L_{PP}/λ increases. Regarding the measured linear forces and moments, they present a similar behaviour as the motions, decreasing as the L_{PP}/λ ratio increases. In regards of the mean second order forces, the

force in surge shows a peak value corresponding to ratios of L_{PP}/λ where the motions in heave and pitch are larger, and roughly a constant values as the ratio L_{PP}/λ increases . A similar behaviour is observed for the sway force, however in this case the maximum amplitude of the sway force is related to maximum roll motions. This correlations to the motions shows the strong dependence of the mean second order forces on the ship motions, and the constant value for larger L_{PP}/λ ratios shows importance of the reflection component in the estimation of the mean second order wave forces. Regarding the variation of the ukc, no significant change in the motions and forces are observed.

From the comparison against the numerical results from the Hydrostar, Seaway, and Wamit, the results shows that linear motions responses are well estimated by all the numerical packages. While in the case of first order forces and the mean wave drift forces, Hydrostar presents a better estimation of the experimental results. Regarding the added wave resistance, the agreement between the experimental results and Seaway can be judged as poor, especially at higher and lower L_{PP}/λ ratios, however, the estimation improve for wave lengths of order of the ship length L_{PP}.

FUTURE WORK

In order to understand better the ship responses under wave action experimental test will be performed with another ship type, e.g. a container ship. The experimental results will be compared against Hydrostar estimations for the linear wave induced motions and forces, and for the mean drift forces. Additionally, to study the added wave resistance, comparison against the methods developed by Faltinsen[7], and the one by Salvesen[8] will be included.

ACKNOWLEDGEMENTS

The research described in this paper is performed in the frame of project WL_2013_47 (Scientific support for investigating the manoeuvring behaviour of ships in waves), granted to Ghent University by Flanders Hydraulics Research, Antwerp (Flemish Government). Part of this work was performed within the project SHOPERA - Energy Efficient Safe SHip OPERAtion, which was partially funded by the EU under contract 605221.

REFERENCES

1. T. H. Havelock, (1942), “Drifting force on a ship among waves”, Philosophical Magazine, vol. 33,.
2. H. Maruo, (1957), “The excess resistance of a ship in a rough seas”, International Shipbuilding Progress, vol. 4, No. 85.
3. W. P. Joosen, (1966), “Added resistance in waves”, 6th Symposium on Naval Hydrodynamics.
4. P. Boese, (1970), “Eine einfache Methode zur Berechnung der Wiederstandserhöhung eines Schiffes in Seegang”, Technical report No. 258, Hamburg, Germany.
5. J. Gerritsma and W. Beukelman, (1972), “Analysis of the resistance increased in waves of a fast cargo ship”, International Shipbuilding Progress, vol. 18, p. 217.
6. J. Strom-Tejsen, H. Y. Yeh, and D. D. Moran, (1973), “Added resistance in waves” SNAME, vol. 81.

7. O. M. Faltinsen, K. Minsaas, N. Liapis, and S. O. Skjørdal, (1980), “Prediction of resistance and propulsion of a ship in a seaway”, The 13th Symposium on Naval Hydrodynamics , pp. 505–529.
8. N. Salvesen, (1978), “Added resistance of ships in waves,” J. Hydrodynamics, Vol. 12, No. 1, pp. 24-34.
9. X. B. Chen, (2005), “Hydrodynamic analysis for offshore LNG terminals,” Second Offshore Hydrodynamics Symposium, Rio de Janeiro, Brazil.
10. F. Rezende, X. Chen, and X. B. Chen, (2007), “Second order loads on LNG terminals in multi-directional sea in water of finite depth”, OMAE, San Diego, USA.
11. S. Sutulo and C. Guedes Soares, (2006), “A unified nonlinear mathematical model for simulating ship manoeuvring and seakeeping in regular waves”, MARSIM, Terschelling, The Netherlands, pp.M-13-1-M13-10.
12. R. Skejic and O. M. Faltinsen, (2007), “A unified seakeeping and maneuvering analysis of two interacting ships”, ICMRT’07, Ischia, Italy, pp.209-218.
13. M.-G. Seo and Y. Kim, (2011), “Numerical analysis on ship maneuvering coupled with ship motion in waves”, Ocean Eng., vol. 38, no. 17–18, pp. 1934–1945.
14. P. A. Bailey, W. C. Price, and P. Temarel, (1998), “A unified mathematical model describing the manoeuvring of a ship travelling in a seaway”, RINA, vol. 140, pp. 131–149.
15. L. Letki and D. A. Hudson, (2005), “Simulation of ship manoeuvring performance in calm water and waves”, University of Southampton, Ship Science Reports, 138, pp.106.
16. Z. Ayaz, D. Vassalos, and O. Turan, (2006), “Parametrical studies of a new numerical model for controlled ship motions in extreme astern seas”, Journal of Marine Science Technology, vol. 11, no. 1, pp. 19–38.
17. R. Skejic, (2008), “Maneuvering and seakeeping of a single ship and of two ships in interaction”, Norwegian University of Science and Technology, PhD. Thesis.
18. H. Yasukawa and Y. Nakayama, (2009), “6-DOF motion simulations of a turning ship in regular waves”, MARSIM, Panama City, Panama.
19. J. M. J. Journée, (2001), “Theoretical manual of SEAWAY”.
20. Bureau Veritas, (2012), “Hydrostar for experts user manual”.
21. C. H. Lee and J. N. Newman, (1999), “WAMIT user manual”.
22. S. De Caluwé, (2015), “Applicability of seakeeping software to predict wave induced forces and motions of ships in shallow water ,” Ghent University, MSc. Thesis.